



# A Full Bayesian Approach to SENSE Image Reconstruction Increases Brain Tissue Contrast and Reduces Noise Leading to More Statistically Significant Task Activation

Chase J. Sakitis<sup>1</sup>, D. Andrew Brown<sup>2</sup> and Daniel B. Rowe<sup>1,3</sup>

<sup>1</sup>Department of Mathematical and Statistical Sciences, Marquette University, Milwaukee, WI, USA

<sup>2</sup>School of Mathematical and Statistical Sciences, Clemson University, Clemson, SC 29634, USA

<sup>3</sup>Department of Biophysics, Medical College of Wisconsin, Milwaukee, WI, USA



## INTRODUCTION

Functional Magnetic Resonance Imaging (fMRI) is a type of medical imaging that was developed in the early 1990's as a technique to noninvasively observe the human brain in action using strong magnetic fields. Historically, a single channel coil receiver has been utilized in fMRI to measure full-sampled  $k$ -space data arrays which are reconstructed into images using the inverse Fourier transform (IFT). Along with parallel utilization of multiple receiver coils, here we use  $n_c = 4$  coils as displayed

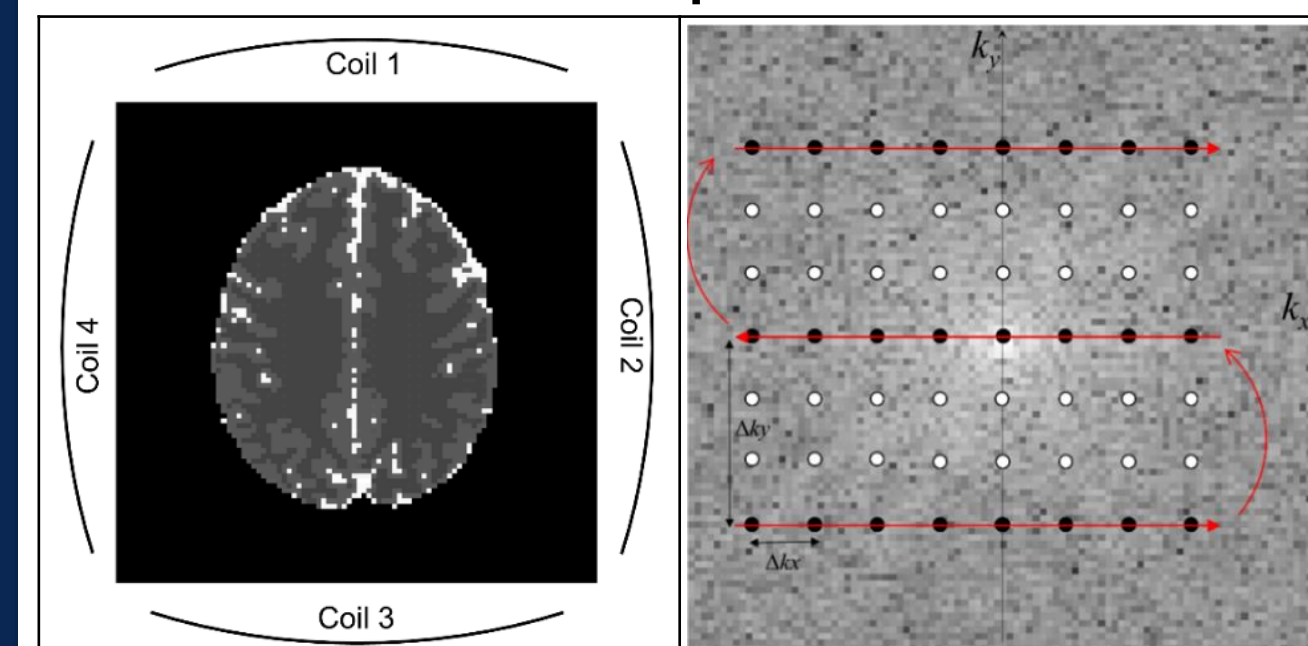


Figure 1: Four channel coil (left) and  $k$ -space zig-zag coverage (right).

in Fig. 1 (left), parallel imaging techniques began subsampling lines in-plane by skipping lines of  $k$ -space for an image causing the reconstructed coil images to be aliased. Skipping lines in  $k$ -space introduces what is called an acceleration factor, or reduction factor. The acceleration

factor indicates which lines of data in  $k$ -space are measured and how many lines are skipped in data acquisition. As shown in Fig. 1 (right), with an acceleration factor of  $n_A = 3$ , every third line horizontally in  $k$ -space is measured by skipping every two lines in the  $k$ -space array. In 1999, Pruessmann et al. introduced SENSitivity Encoding (SENSE) which operates on the aliased images after the IFT [1].

## SENSE

Each local receiver coil possesses a depth sensitivity profile that is related to its size measuring a different sensitivity weighted version of the true slice. Depicted in Fig. 2 (center) is a true slice image with  $n_A = 3$  voxels  $v_1, v_2, v_3$  in corresponding locations relative to each strip [2]. Each coil measures a rectangular  $k$ -space array that after IFT reconstruction produces an aliased image that is the weighted sum of three horizontal strips of the full true image. In Fig. 2 (top right), the true aliased image is the pointwise multiplication of the given voxel by the sensitivity profile for coil 1 summed for the three strips. This process is the same for the other

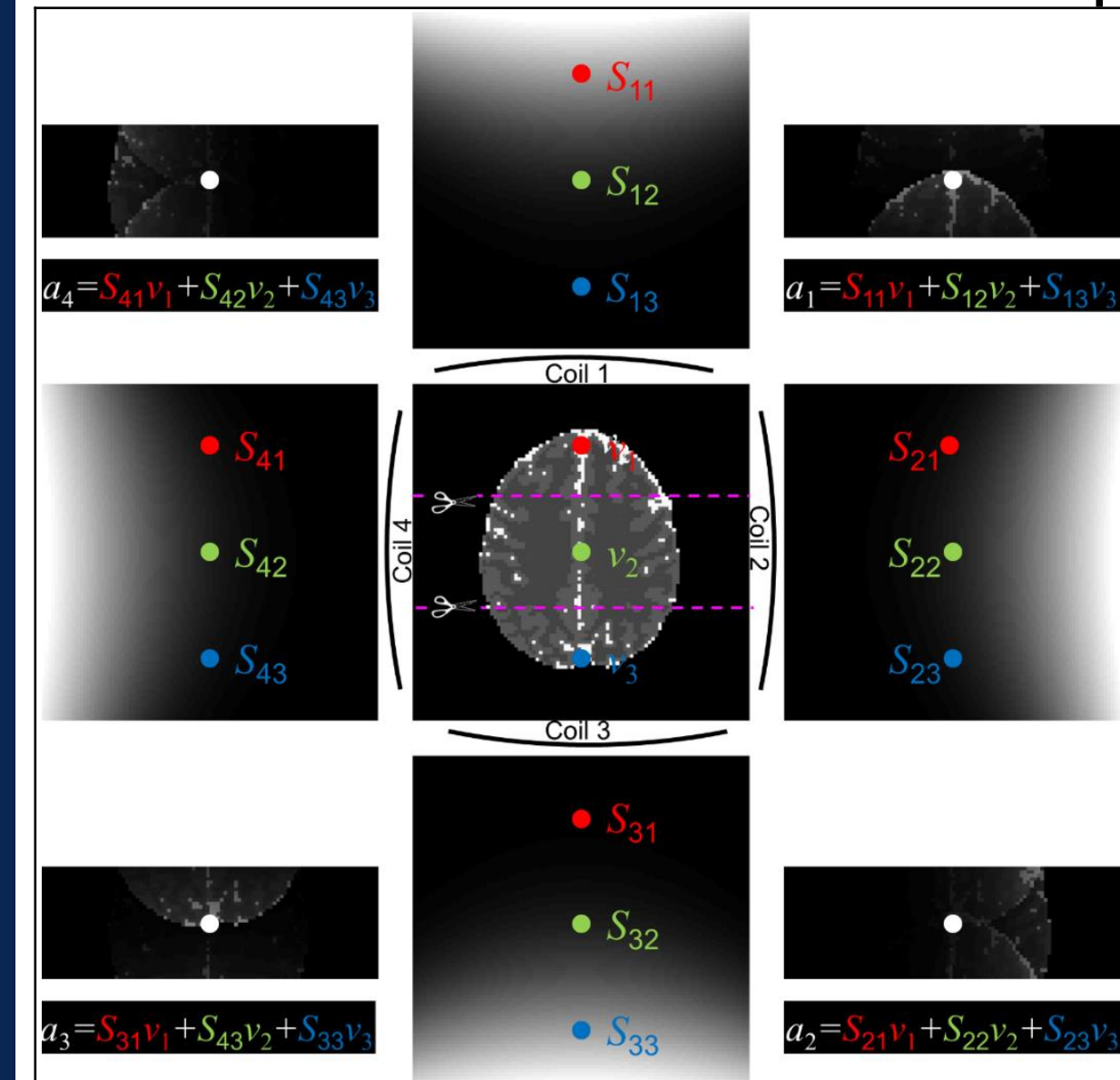


Figure 2: True slice image (center) along with coil sensitivity profiles (left, right, top, bottom) and sensitivity weighted true aliased images (corners).

3 coils creating a system of equations shown in Eq. 1.

$$\begin{bmatrix} a_1 \\ a_2 \\ a_3 \\ a_4 \end{bmatrix} = \begin{bmatrix} S_{11} & S_{12} & S_{13} \\ S_{21} & S_{22} & S_{23} \\ S_{31} & S_{32} & S_{33} \\ S_{41} & S_{42} & S_{43} \end{bmatrix} \begin{bmatrix} v_1 \\ v_2 \\ v_3 \end{bmatrix} \quad (1)$$

Which can be represented as

$$a = Sv \quad (2)$$

and solved using the least squares estimate in Eq 3.

$$\hat{v} = (S^T S)^{-1} S^T a \quad (3)$$

This parameter estimation approach can be difficult because the design matrix, generally, is ill-conditioned meaning it is not positive definite. There are numerous methods to correcting the rank deficiency in the design matrix, however, these methods could result in valuable data being unused, limitation of useful results, or can be more computationally expensive. These flaws become the main motivation for a Bayesian approach to SENSE (BSENSE) that allows for a more general process for image reconstruction.

## BSENSE

The  $k$ -space arrays acquired by the MRI scanner are complex-valued which means after the IFT, the aliased coil measurements would also be complex-valued. This would indicate that the  $a$ ,  $S$ , and  $v$  in Eq. 2 are complex-valued parameters, so the SENSE parameter estimation remains in complex form. For BSENSE, we can represent Eq. 2 by a real-valued isomorphic representation [3] of the complex model, shown in Eq. 4.

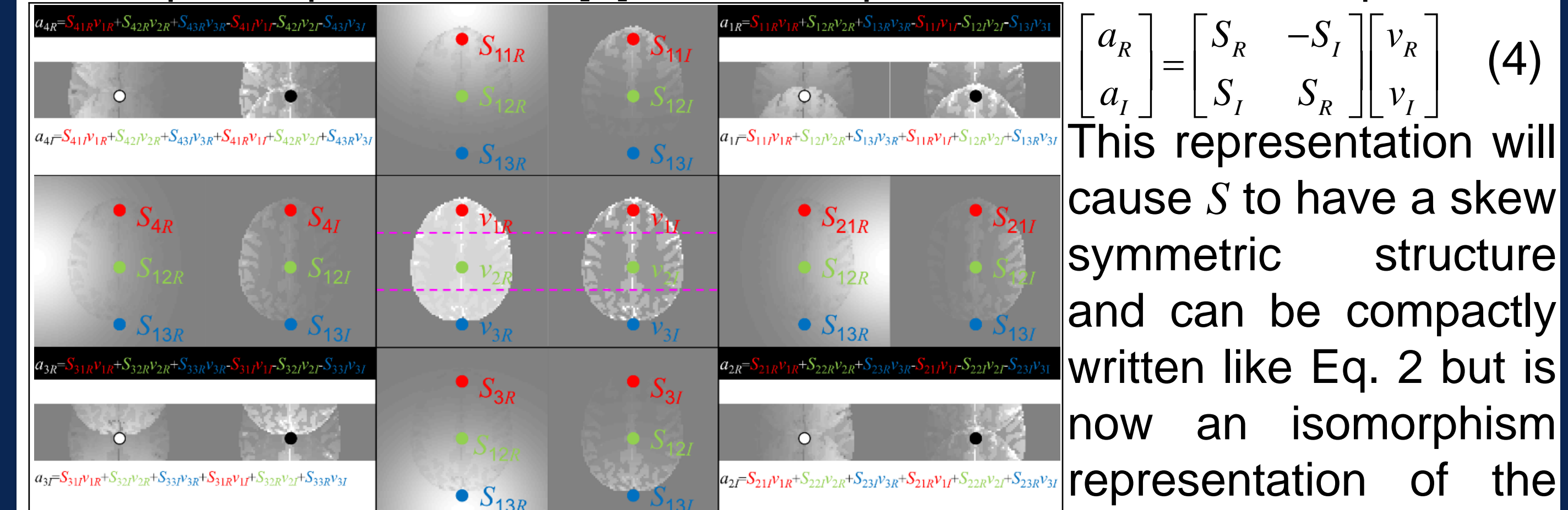


Figure 3: True slice complex-valued image (center) along with complex-valued coil sensitivity profiles (left, right, top, bottom) and complex-valued sensitivity weighted true aliased images (corners).

$$\begin{bmatrix} a_R \\ a_I \end{bmatrix} = \begin{bmatrix} S_R & -S_I \\ S_I & S_R \end{bmatrix} \begin{bmatrix} v_R \\ v_I \end{bmatrix} \quad (4)$$

This representation will cause  $S$  to have a skew symmetric structure and can be compactly written like Eq. 2 but is now an isomorphism representation of the complex equation. With the Bayesian approach, prior distributions are provided for the unknown parameters and valuable available prior information is utilized for parameter estimation. Using Eq. 2 with added measurement error, our model becomes:

$$a = Sv + \varepsilon \quad (5)$$

where  $a \in \mathbb{R}^{2n_c \times 1}$ ,  $S \in \mathbb{R}^{2n_c \times 2n_A}$ ,  $v \in \mathbb{R}^{2n_A \times 1}$ ,  $\varepsilon \in \mathbb{R}^{2n_c \times 1}$ , and  $\varepsilon \sim N(0, \sigma^2 I_{n_c})$ . The likelihood distribution of the measurements is

$$p(a | S, v, \sigma^2) \propto (\sigma^2)^{-2n_c} \exp \left[ -\frac{1}{2\sigma^2} (a - Sv)^T (a - Sv) \right] \quad (6)$$

where  $a$  is the observed aliased coil image measurements,  $S$  is the unobserved coil reception sensitivities,  $v$  is the unobserved true image slice voxel values, and  $\sigma^2$  is the unobserved image noise variance. We can quantify available prior information about the unobserved parameters  $S$ ,  $v$ , and  $\sigma^2$  with assessed hyperparameters of the prior distributions fusing information contained in pre-scan calibration images.

$$p(H | n_s, H_0, \sigma^2) \propto (\sigma^2)^{-2n_s} \exp \left[ -\frac{n_s}{2\sigma^2} \text{tr}[(H - H_0)^T (H - H_0)] \right], \quad (7)$$

$$p(v | n_v, v_0, \sigma^2) \propto (\sigma^2)^{-2n_v} \exp \left[ -\frac{n_v}{2\sigma^2} (v - v_0)^T (v - v_0) \right], \quad (8)$$

$$p(\sigma^2 | \alpha, \beta) \propto (\sigma^2)^{-(\alpha+1)} \exp \left[ -\frac{\beta}{\sigma^2} \right]. \quad (9)$$

Using the  $H = [S_R^T \ S_I^T]$  representation of the sensitivities will ensure that the real and imaginary components only get estimated once, preserving the proper skew symmetry constraint of the  $a$  posteriori estimated sensitivities which was previously not done [2]. The Maximum A Posteriori (MAP) was estimated using the Iterated Conditional Modes (ICM) optimization algorithm [4] with equations 10, 11, and 12 showing the conditional modes used for the algorithm.

$$\sigma_{MAP}^2 = \frac{(a - Sv)^T (a - Sv) + n_s (v - v_0)^T (v - v_0) + n_s \text{tr}[(H - H_0)^T (H - H_0)] + \alpha \beta}{2(2n_c + 2n_A + \alpha + 2n_s n_A + 1)} \quad (10)$$

$$H_{MAP} = (C^T C + n_s I_{2n_s})^{-1} (C^T Y + n_s H_0) \quad (11)$$

$$v_{MAP} = (S^T S + n_s I_{2n_A})^{-1} (S^T a + n_s v_0) \quad (12)$$

The MCMC Gibbs sampler [5] was implemented with posterior conditional distributions to form a chain of reconstructed posterior conditional images.

$$\sigma^2 | v, S, a \sim \text{IG}(\alpha, \beta) \quad (13)$$

$$H | v, \sigma^2, a \sim \text{MN}(\hat{H} = (C^T C + n_s I_{2n_s})^{-1} (C^T Y + n_s H_0), I_{n_s}, \sigma^2 (C^T C + n_s I_{2n_s})^{-1}) \quad (14)$$

$$v | S, \sigma^2, a \sim N(\hat{v} = (S^T S + n_s I_{2n_A})^{-1} (S^T a + n_s v_0), \sigma^2 (S^T S + n_s I_{2n_A})^{-1}) \quad (15)$$

$$C = \begin{bmatrix} v_R^* & -v_I^* \\ v_I^* & v_R^* \end{bmatrix} \quad Y = \begin{bmatrix} a_R \\ a_I \end{bmatrix} \quad H_0 = \begin{bmatrix} S_{0R} & S_{0I} \end{bmatrix} \quad v_0 = \begin{bmatrix} v_{0R} \\ v_{0I} \end{bmatrix}$$

## RESULTS

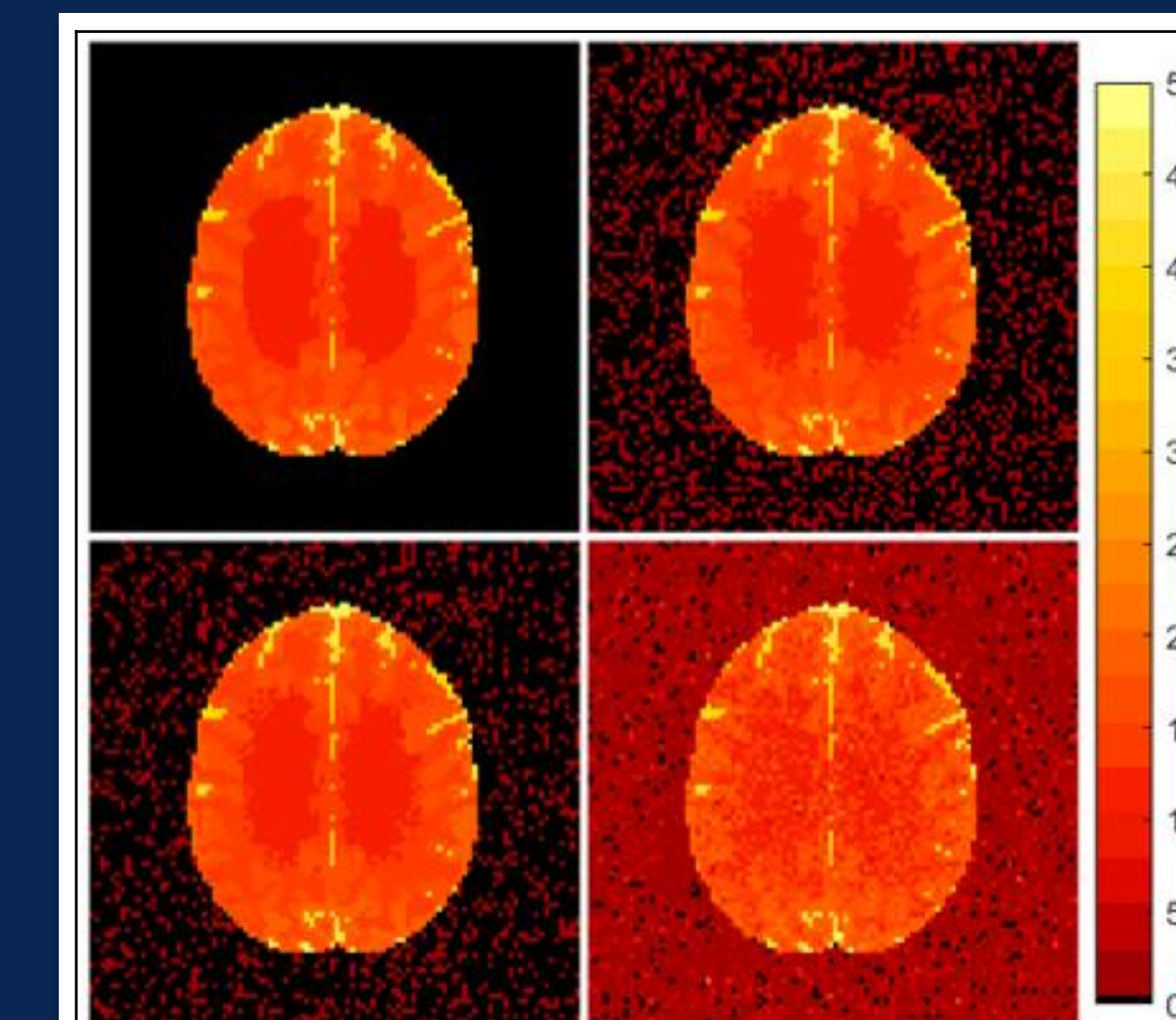


Figure 4: True non-task unaliased image (top left), BSENSE MAP unaliased non-task magnitude image (top right) using ICM, Mean BSENSE unaliased non-task magnitude image (bottom left) using Gibbs sampling, and SENSE non-task magnitude image (bottom right).

These techniques were applied to simulated data and compared to SENSE as shown in Fig. 4. We can see that the joint MAP estimate and marginal posterior mean for BSENSE image reconstruction produce images with no aliasing artifacts and clearer brain tissue contrast when compared to SENSE. The objective of fMRI is to have the patient perform a task, finger tapping, and observe the working brain where increased neuronal activation occurs. The non-task reconstructed images create a baseline value for each voxel

giving us an intercept only simple linear regression  $y = \beta_0$ , where  $y$  is the estimated voxel value. By adding task activation to certain images in the series, we then have a simple linear regression  $y = \beta_0 + x\beta_1$  for our estimated voxel values. In this regression,  $\beta_0$  is the baseline voxel value from the non-task reconstructed images determining the signal-to-noise ratio (SNR), which is  $\beta_0/\sigma$ , and  $\beta_1$  is the estimated increase from  $\beta_0$  which would be the contrast-to-noise ratio (CNR), calculated by  $\beta_1/\sigma$ . The vector  $x$  consists of zeros and ones where the zeros correspond to images in the series without task activation and ones corresponding to images with task activation. Since CNR is often notably lower than SNR with noise generally present, the activation is not usually visual on the final reconstructed image. Instead, a hypothesis test is carried out with  $\beta_1 \leq 0$  as the null hypothesis and  $\beta_1 > 0$  as the alternative hypothesis. A one-tailed  $t$ -test is implemented to determine if any of the voxels experienced statistically significant increase from the performed task. The true noiseless non-task image and task image was used to generate a series of 512 simulated aliased coil images by alternating between 8 task and 8 non-task images, mimicking a real-world fMRI experimental process. The entire series was reconstructed into full, unaliased images using both

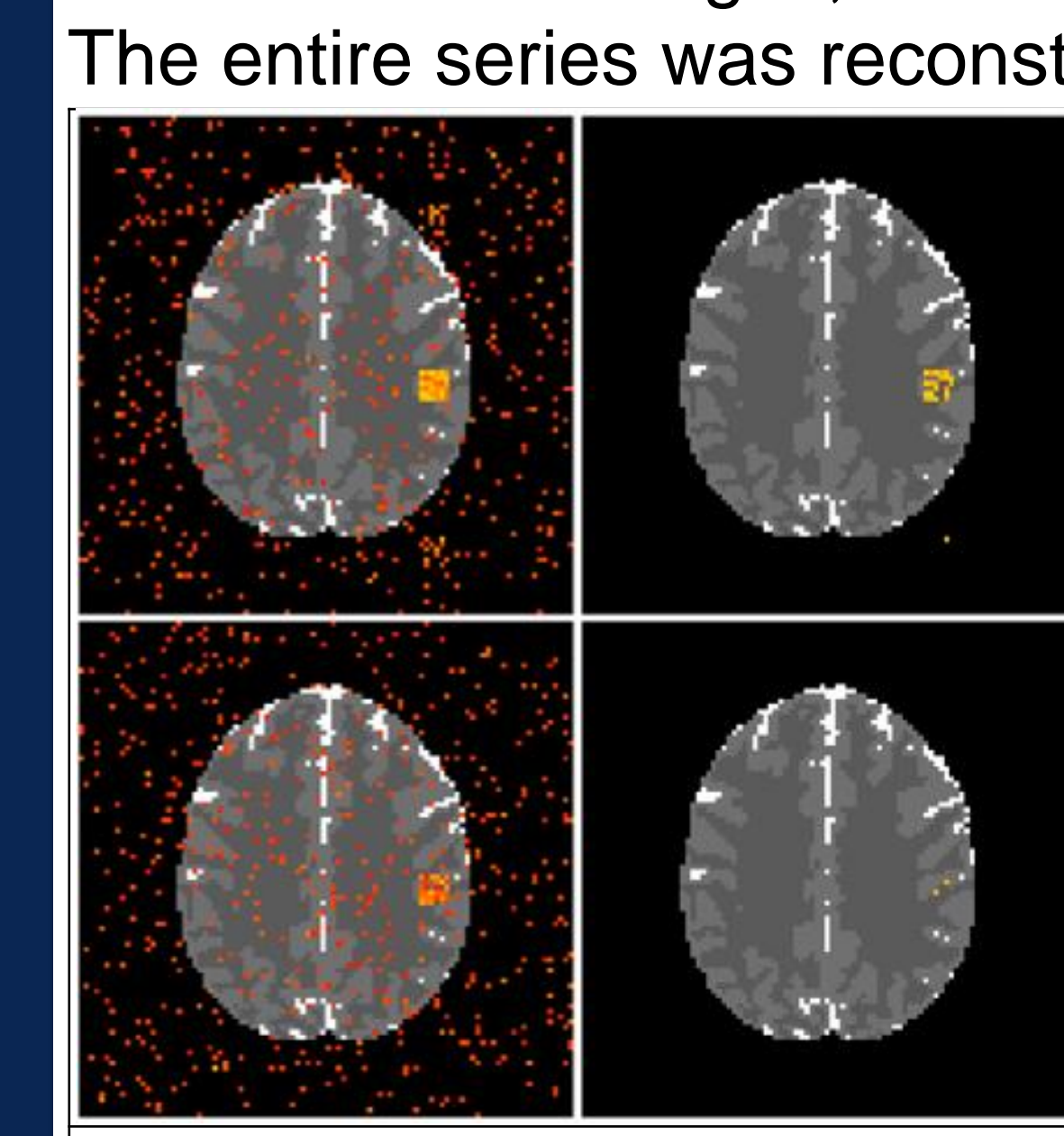


Figure 5: Statistically significant voxels using PCER for BSENSE reconstructed images (top left), significant voxels using FDR for BSENSE (top right), significant voxels using PCER for SENSE (bottom left), and significant voxels using FDR for SENSE (bottom right).

SENSE and BSENSE MAP separately. Then the hypothesis test was utilized with a 0.1 significance level to determine voxels with a statistically significant signal increase. In Fig. 5, the left column shows the statistically significant voxels using the per-comparison error rate (PCER) and the right column shows the significant voxels using the false discovery rate (FDR) correction with BSENSE on top and SENSE on bottom for both columns. We can see that the BSENSE MAP estimate performed better at detecting task activation after the multiplicity correction.

## REFERENCES

- (1) KP Pruessmann et al. *SENSE: Sensitivity Encoding for fast MRI*. MRM 42:952-962, 1999.
- (2) Rowe DB. *A Bayesian approach to SENSE Image Reconstruction in fMRI*. Proc. Joint Stat Meet, Statistical Society of Canada, 21:378-92, Baltimore, MD, 2017.
- (3) Bruce IP, Karaman MM, Rowe DB. *A statistical examination of SENSE image reconstruction via an isomorphism representation*. Magn Reson Imaging, 29:1267-87, 2011.
- (4) Lindley DV, Smith AFM. *Bayes estimates for the linear model*, J Royal Stat Soc B, 34:1-18, 1972.
- (5) Geman S, Geman D. *Stochastic Relaxation, Gibbs Distributions, and the Bayesian Restoration of Images*. IEEE Trans Pattern Anal Mach Intell, 6:721-41, 1984.